American Journal of Mechanics and Applications
2026, Vol. 13, No. 1, pp. 10–21
https://doi.org/10.11648/j.ajma.20261301.12

SciencePG
Science Publishing Group

Research Article

Rolling Window Deep Learning for Hard-rock TBM Penetration Rate Prediction

Nantapol Monthanopparat*, Tawatchai Tanchaisawat

Department of Civil Engineering, Chiang Mai University, Chiang Mai, Thailand

Abstract

Penetration rate prediction for hard rock tunnel boring machines (TBMs) remains challenging because rock mass conditions and machine operating regimes vary continuously along the tunnel alignment. Conventional static prediction models may not adequately represent such non-stationary construction conditions, particularly when geotechnical measurements are incomplete or obtained with delay during excavation. This study aims to develop a construction-phase prediction framework for ring-scale TBM penetration rate in a granite tunnel drive by integrating geotechnical data completion, sequence deep learning, and rolling-window model evaluation. A dataset of 1,000 consecutive rings was compiled, including boring-only penetration rate, thrust, torque, cutterhead rotational speed, rock mass type, and uniaxial compressive strength (UCS). Missing UCS measurements were completed using inverse distance weighting within a block model representation, resulting in estimated UCS values of approximately 33–177 MPa for rock masses dominated by massive and fractured granite. Three sequence deep learning models, namely long short-term memory (LSTM), gated recurrent unit (GRU), and temporal convolutional network (TCN), were evaluated using root mean square error (RMSE), mean absolute error (MAE), and a symmetric ±10% tolerance band adapted from accuracy-band concepts used in AACE-based project controls. The proposed rolling protocol used 100-ring validation and 100-ring test blocks to assess predictive performance under changing ground conditions. The results show that the optimized GRU model provided the most robust overall performance, achieving a mean test RMSE of approximately 0.229 m/h and a mean within-band compliance of approximately 54% across rolling folds. These findings indicate that rolling-window sequence learning can provide a practical and adaptable framework for construction-phase TBM performance prediction under evolving geological and operational conditions.

Keywords

Tunnel Boring Machine, Penetration Rate Prediction, Hard Rock Tunnelling, Rolling Window Evaluation, Gated Recurrent Unit

1. Introduction

Penetration rate is a primary driver of production efficiency and schedule performance in hard rock tunnel boring machine operations, and reliable construction phase prediction remains challenging in practice [1]. Along a tunnel alignment, rock mass conditions and operating regimes evolve in response to lithological variability, fracture intensity, and operational adjustments. These changes introduce non stationarity at ring scale and can cause significant deviations between planned and actual advance, particularly when excavation transitions from intact granite to highly fractured or faulted granite [2].

*Correspondence: Nantapol Monthanopparat (nantapol_mon@cmu.ac.th)

Received: 4 May 2026; **Accepted:** 14 May 2026; **Published:** 26 May 2026

Rock mechanics practice has long relied on empirical and semi theoretical performance models to estimate hard rock tunnel boring machine penetration rate and to inform construction planning [3]. While these models provide interpretable relationships between machine inputs and rock mass strength descriptors, their continuous application during construction is frequently constrained by incomplete geotechnical data and calibration needs that are sensitive to local ground and operational conditions [4]. In shielded tunnel boring machine operations, continuous measurement of rock properties at the face is often impractical, and strength information such as uniaxial compressive strength is commonly sparse or discontinuous along chainage, which limits model applicability across variable rock mass regimes [5]. A previous project specific assessment on a granite tunnel boring machine drive in Northern Thailand reported root mean square errors of 0.356 to 0.893 meters per hour across a set of commonly used penetration rate models, indicating that prediction accuracy can be highly variable when applied under evolving rock mass and operational conditions [6]. Table 1 summarizes this performance range and provides context for a construction-oriented evaluation framework. In addition, the practical use of these existing models was constrained by incomplete geotechnical inputs at ring scale. Although the evaluation interval spans Ring No. 3415 to Ring No. 5011, only 173 ring datasets contained sufficient inputs for model execution, comprising 123 datasets in RMT2 and 50 datasets in RMT2F or RMT2S.

Recent advances in data driven modelling provide an alternative route for construction phase prediction by learning relationships directly from operational monitoring data [7]. For tunnel boring machine performance, sequence models are especially relevant because ring scale penetration rate exhibits temporal dependence and regime transitions. However, for non-stationary tunnelling data, a key practical question is not only whether a model achieves low error on a single train test division, but whether it retains reliability when trained on earlier segments and evaluated on later segments that may contain different rock mass regimes.

This paper presents a construction phase prediction framework for hard rock tunnel boring machine penetration rate in a granite tunnel boring machine drive in Northern Thailand, emphasizing expanding rolling window evaluation. Ring scale boring only penetration rate is modelled using thrust, torque, cutterhead rotational speed, rock mass type, and uniaxial compressive strength. Because strength measurements are incomplete along the alignment, missing uniaxial compressive strength values are completed using inverse distance weighting within a block model representation to support a consistent evaluation scenario [8]. Model performance is assessed using root mean square error and mean absolute error together with a symmetric plus or minus ten percent tolerance band adapted from accuracy band concepts used in AACE based project controls [9]. The expanding rolling protocol uses one hundred ring validation and one hundred ring test blocks to quantify robustness across chainage, and sequence deep learning models including long short-term memory, gated recurrent unit, and temporal convolutional network are evaluated. The framework supports transparent construction phase model selection across granite, highly fractured granite, and faulted granite regimes.

Table 1. *Summary of prediction performance of existing penetration rate models in a granite TBM drive in Northern Thailand [6].*

Model	Author	RMSE		
		All RMT	RMT2	RMT2F/2S
CSM	Rostami, J. [10]	0.499	0.356	0.743
MCSM	Yagiz, S. [11]	0.690	0.764	0.460
Yagiz	Yagiz, S. [12]	0.438	0.430	0.457
NTNU	Bruland, A. [13]	0.816	0.787	0.885
Modified NTNU	Macias, F. J. [5]	0.809	0.787	0.861
Gehring	Gehring, K. [14]	0.629	0.481	0.893
Alpine by Wilfing	Wilfing, L. [15]	0.514	0.390	0.736
Farrokh	Farrokh, E. et al. [4]	0.444	0.422	0.493

*RMSE-Root means square errors, RMT-Rock mass type, RMT2-Granite (massive) and RMT2F/2S-Highly fractured granite/Faulted granite.

2. Project Background and Geological Setting

2.1. Project Overview and Data Scope

The case study is part of a water transfer tunnel project in Northern Thailand with the objective of diverting water from the Mae Tang River to the Mae Ngad Reservoir. The investigated TBM-driven segment is 9.7 km long, and this paper focuses on a continuous ring interval from Ring No. 2350 to Ring No. 3349, corresponding to 1,000 consecutive rings. Each ring represents 1.4 m of advance. Figure 1 provides the anonymized location and simplified alignment of the granite TBM drive, and Figure 2 shows the geological zoning along the alignment.

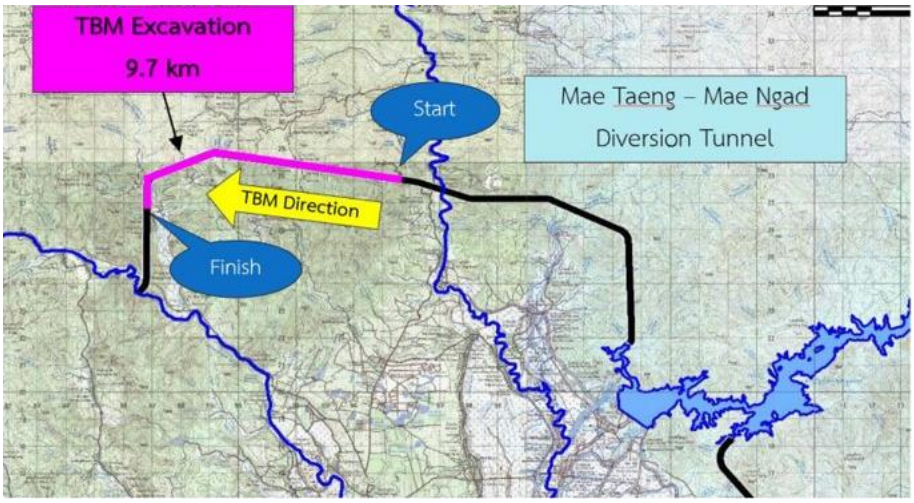

Figure 1. *Location and simplified alignment schematic of a granite TBM drive in Northern Thailand used as the case study.*

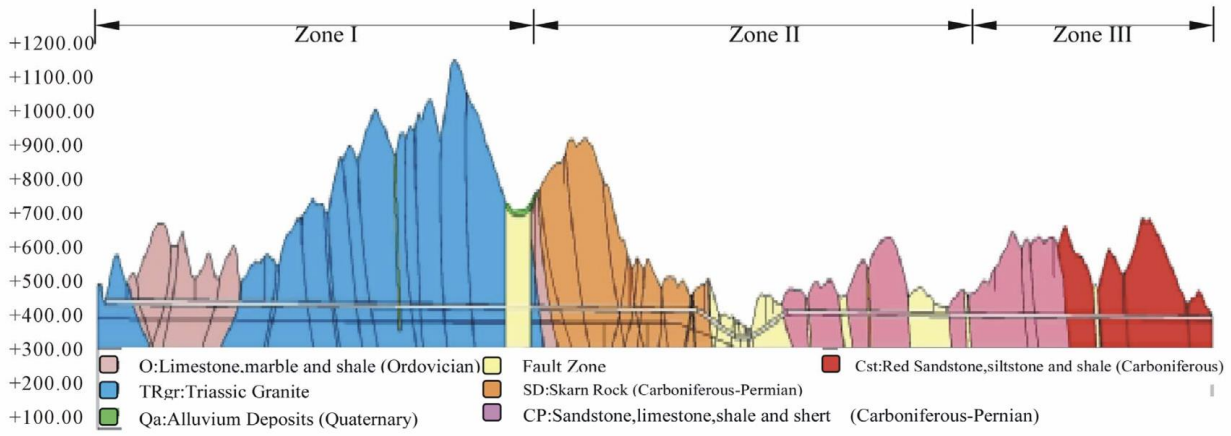

Figure 2. *Geological zoning along the tunnel alignment showing three geological zones for the studied granite TBM drive in Northern Thailand adapted from the previous manuscript based on the work of Kaewkongkaew and co-authors [16].*

2.2. TBM System and Excavation Setup

Excavation was performed using a double shield hard rock TBM. The key specifications relevant to the modelling inputs are summarized in Table 2, including excavation diameter, cutter-head configuration, maximum thrust capacity, and cutterhead rotational speed range. Operational variables used in the predictive models are derived from ring aggregated TBM monitoring records.

Table 2. *Double shield TBM specification.*

Item	Specification
TBM type	Double shield TBM
Excavation diameter	4.74 m.
Cutter discs	32 discs

Item	Specification
Disc diameter	17 inches (432 mm.)
Average cutter spacing	82 mm.
Maximum thrust	7,500 kN.
Cutterhead rotation speed	5.0-9.0 rpm
Backup system	Rolling stock for material supply and muck hauling

2.3. Geological Setting and Rock Mass Type Classification

The tunnel alignment is divided into three geological zones and TBM excavation is mainly associated with Zone I where granite and marble occur with localized intervals of intense fracturing and fault influence. Figure 2 presents this zonation context, while Figure 3 shows the rock mass type log along Ring No. 2350 to Ring No. 3349.

Rock mass variability is represented using three rock mass type categories derived from construction geology records: RMT2 granite, RMT2F highly fractured granite, and RMT2S fault-ed granite. Representative field observations for each class are shown in Figure 4. Uniaxial compressive strength is used as the intact rock strength descriptor. Because UCS measurements are incomplete at ring scale in shielded TBM operations, UCS is treated under Scenario A by completing missing measurements using inverse distance weighting within a block model representation to obtain continuous ring scale UCS estimates [8]. Table 3 summarizes the dataset composition and descriptive statistics of boring only penetration rate and UCS estimates by rock mass type.

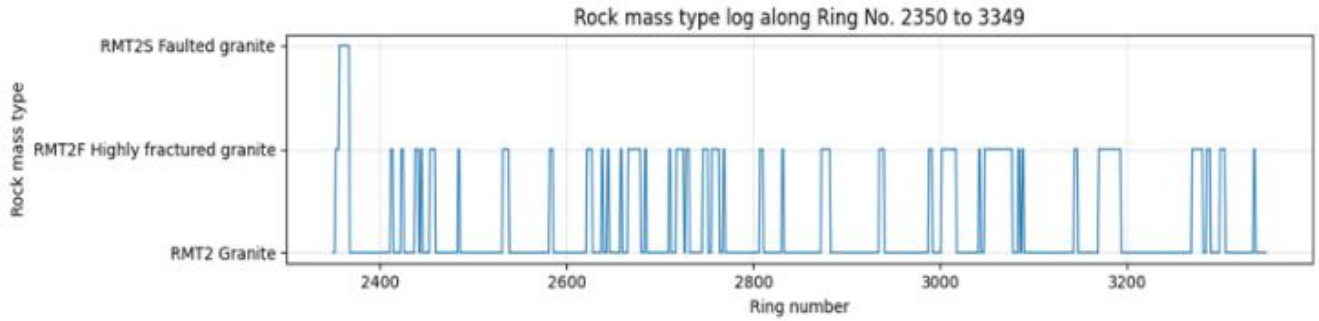

Figure 3. Rock mass type log along Ring No. 2350 to 3349 showing transitions between RMT2 granite RMT2F highly fractured granite and RMT2S faulted granite supporting rolling window evaluation under chainage dependent non stationarity.

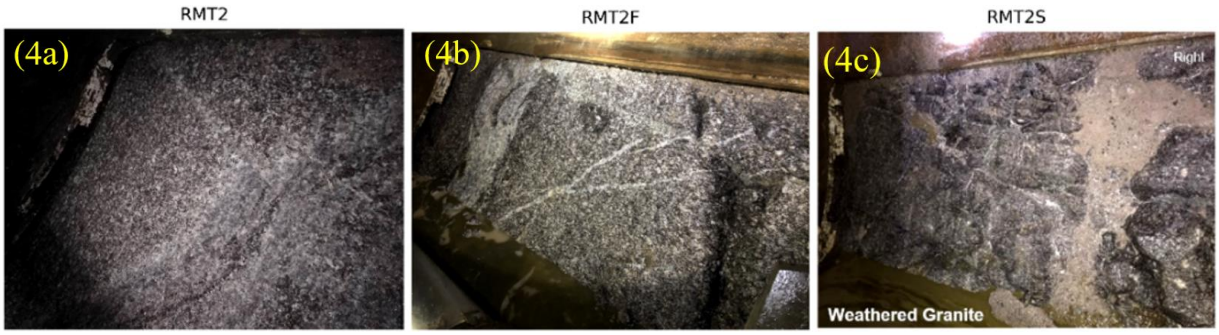

Figure 4. Representative rock mass observations recorded at the TBM tail shield opening for the three rock mass types used in this study (a) RMT2 granite at Ring No. 2527 (b) RMT2F highly fractured granite at Ring No. 2884 and (c) RMT2S faulted granite at Ring No. 2357.

Table 3. Summary statistics of boring only penetration rate and UCS by rock mass type for the 1,000-ring dataset covering No. 2350 to 3349.

Rock Mass Type	Number (n.)	Boring-only Penetration rate (m/h)			UCS Measure and Estimated, MPa.		
		means	Min.	Max.	means	Min.	Max.
2	766	1.218	0.180	2.313	94.59	55.16	173.62
2F	233	1.556	0.588	4.249	86.39	40.81	112.46

Rock Mass Type	Number (n.)	Boring-only Penetration rate (m/h)			UCS Measure and Estimated, MPa.		
		means	Min.	Max.	means	Min.	Max.
2S	11	1.239	0.817	2.098	100.04	32.91	177.00
All	1000	1.293	0.180	4.249	92.82	32.91	177.00

3. Data and Preprocessing

3.1. Ring Scale Dataset

The analysis uses ring scale records for Ring No. 2350 to Ring No. 3349, comprising 1,000 consecutive rings. Each record contains ring aggregated operational variables, geological descriptors, and the response variable for penetration rate prediction.

3.2. Response Variable

The response variable is boring only penetration rate expressed in meters per hour and aggregated per ring.

3.3. Input Features and Missing Geological Information

Model inputs include average thrust, average torque, and average cutterhead rotational speed per ring, together with rock mass type and uniaxial compressive strength. In shielded TBM excavation, UCS and geology measurements are often incomplete at ring scale due to limited face access and discrete investigation coverage. Figure 5 illustrates the typical mismatch between discrete borehole information and continuous ring scale excavation records. To enable consistent evaluation under Scenario A, missing UCS measurements are completed using inverse distance weighting within a block model representation to provide continuous ring scale UCS estimates [8].

3.4. Encoding and Normalization

Rock mass type is encoded using one hot representation of RMT2, RMT2F, and RMT2S (Table 4). Continuous variables are standardized using parameters computed from the training portion of each rolling fold and then applied to the corresponding validation and test blocks to avoid information leakage across chainage.

3.5. Sequence Construction

Each sample is formed using a sliding window of prior rings containing the operational variables, one hot rock mass type encoding, UCS estimates, and lagged penetration rate. The target is penetration rate for the subsequent ring.

3.6. Stage 1 and Stage 2 Datasets

Stage 1 uses 500 rings for exploratory comparison of sequence deep learning architectures. Stage 2 uses the full 1,000 ring dataset for expanding rolling window evaluation with 100 ring validation and 100 ring test blocks and supports tolerance band assessment as described in the methodology.

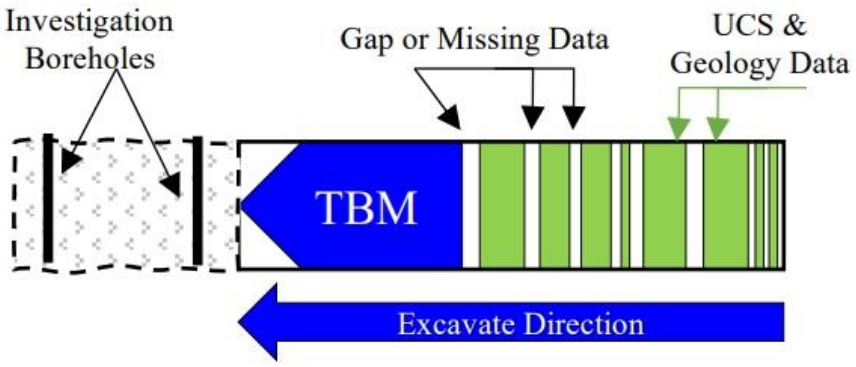

Figure 5. *Conceptual illustration of investigation boreholes and ring scale gaps in UCS and geology data during shielded TBM excavation showing why UCS completion is required for construction phase modelling [6].*

Table 4. One hot encoding scheme for rock mass type.

Rock mass type	One hot encoding		
RMT2 Granite	1	0	0
RMT2F Highly fractured granite	0	1	0
RMT2S Faulted granite	0	0	0

4. Methodology

This section describes the staged evaluation design, the expanding rolling protocol, the evaluation sequence models, and the performance criteria used for model selection under construction phase non stationarity.

4.1. Stage 1 and Stage 2 Evaluation Design

Stage 1 is used for exploratory comparison on 500 rings with a time ordered split into training, validation, and test subsets of 70 percent, 15 percent, and 15 percent, respectively.

Stage 2 applies an expanding rolling window evaluation over the 1,000-ring dataset, using 100 ring validation and 100 ring test blocks advanced in 100 ring steps. The fold definitions are summarized in Table 5 and ensure that validation and test blocks always occur after the training segment in ring order to avoid temporal leakage [17].

4.2. Sequence Deep Learning Models

Three sequence models are evaluated: long-short term memory [18], gated recurrent unit [19], and temporal convolutional network [20]. Models predict next ring penetration rate using a fixed length input window of historical rings containing operational variables, one hot rock mass type encoding, UCS estimates under Scenario A, and lagged penetration rate. LSTM is used as a reference gated recurrent model, GRU as a compact recurrent alternative, and TCN as a causal convolutional sequence model.

4.3. Lightweight Hyperparameter Optimization

Stage 2 includes a lightweight grid-based optimization for recurrent models under rolling evaluation. Candidate configurations are ranked using rolling mean RMSE, MAE, and tolerance band compliance. The search space is summarized in Table 6.

Table 5. Expanding rolling window folds for Stage 2 Evaluation.

Fold	Training rings (n.)	Validation rings (n.)	Test rings (n.)
1	Ring No. 2350 to 2849 (500)	Ring No. 2850 to 2949 (100)	Ring No. 2950 to 3049 (100)
2	Ring No. 2350 to 2949 (600)	Ring No. 2950 to 3049 (100)	Ring No. 3050 to 3149 (100)
3	Ring No. 2350 to 3049 (700)	Ring No. 3050 to 3149 (100)	Ring No. 3150 to 3249 (100)
4	Ring No. 2350 to 3149 (800)	Ring No. 3150 to 3249 (100)	Ring No. 3250 to 3349 (100)

Table 6. Hyperparameter Search Space for Lightweight Optimization.

Item	Value tested
Input window length W (rings)	10, 20
Recurrent hidden units	32, 64
Dropout	0.1, 0.2
Learning rate	1e-3, 5e-4

4.4. Evaluation Metrics and Tolerance Band

Let y_i denote the observed penetration rate and $\hat{y}_i$the predicted penetration rate for n samples in a validation or test block. RMSE and MAE are computed as:

$$RMSE = \sqrt{\frac{\sum_{i=1}^{N}(\hat{y}_i - y_i)^2}{n}} \quad (1)$$

$$MAE = \frac{1}{n}\sum_{i=1}^{n}|y_i - \hat{y}_i| \quad (2)$$

A symmetric tolerance band is computed as the percentage of predictions satisfying.

$$\left|\frac{\hat{y}_i - y_i}{y_i}\right| \leq 0.10, \quad (3)$$

With within band compliance defined as:

$$WithinBand_{\pm 10\%} = \frac{1}{n}\sum_{i=1}^{n} \left\| \left(\left|\frac{\hat{y}_i - y_i}{y_i}\right| \right) \times 100\% \quad (4)$$

This criterion is adapted from accuracy band concepts used in AACE based project controls and is reported overall and by rock mass type [9].

5. Results

This section summarizes the staged results of the proposed framework. Existing penetration rate model performance and data availability constraints provide motivation (Table 1). Stage 1 reports an exploratory comparison of the sequence models on 500 rings (Table 7). Stage 2 reports expanding rolling evaluation across chainage and the outcomes of lightweight optimization, including tolerance band compliance (Figure 6 to Figure 12 and Table 8).

5.1. Existing Model Performance and Data Availability Constraints

Table 1 summarizes the previously reported prediction performance of commonly used penetration rate models for a granite TBM drive in Northern Thailand. In addition to performance variability, model execution at ring scale was constrained by incomplete geotechnical inputs. Although the evaluation interval spanned Ring No. 3415 to Ring No. 5011, only 173 ring datasets contained sufficient inputs for model execution, comprising 123 datasets in RMT2 and 50 datasets in RMT2F or RMT2S. This motivates the present rolling window framework using ring scale monitoring data with Scenario A UCS completion.

5.2. Stage 1 Exploratory Comparison on 500 Rings

Stage 1 provides an exploratory comparison of LSTM, GRU, and TCN on 500 rings using a time ordered split as described in Section 4.1. Table 7 summarizes Stage 1 test performance and indicates that sequence models can represent ring scale penetration rate behavior using operational inputs together with rock mass type and UCS estimates under Scenario A.

5.3. Stage 2 Expanding Rolling Window Evaluation Across Chainage

Stage 2 applies the expanding rolling protocol in Table 5 to quantify robustness across chainage under non stationarity [17]. Geological variability is contextualized by Figure 2 and Figure 3, while Table 3 summarizes dataset composition by rock mass type. Fold wise test performance of LSTM, GRU, and TCN is shown in Figure 6 to Figure 8 for RMSE, MAE, and within band compliance, demonstrating substantial fold dependence and segment specific variation.

5.4. Lightweight Optimization and Selected Configuration

A lightweight optimization is conducted within the search space in Table 6. Table 8 reports the top ranked recurrent configurations and their rolling mean performance. Figure 9 and Figure 10 summarize the trade-off between mean test RMSE and tolerance band compliance for GRU and LSTM configurations, respectively. The best ranked configuration is a GRU model with input window length 10 rings, 32 hidden units, dropout 0.2, and learning rate 1e-3, achieving mean test RMSE 0.229 m/h, mean test MAE 0.157 m/h, and mean within band compliance 53.75 per-cent across rolling folds.

5.5. Regime Aware Results by Rock Mass Type

Table 7. Stage 1 performance summary of sequence deep learning models on the 500-ring dataset.

Model	All RMT		RMT2			RMT2F		
	RMSE	MAE	n	RMSE	MAE	n	RMSE	MAE
LSTM	0.151	0.105	59	0.151	0.107	6	0.152	0.090
GRU	0.153	0.114	59	0.146	0.110	6	0.212	0.156
TCN	0.189	0.147	59	0.196	0.154	6	0.105	0.081

Regime aware results are summarized by rock mass type using Figure 11 for mean test RMSE and Figure 12 for mean within band compliance across rolling folds. Figure 4 provides representative rock mass observations for each class, and Figure 5 illustrates the origin of UCS data gaps that motivate Scenario A completion. RMT2S results should be interpreted cautiously due to limited sample representation in the analyzed interval (Table 3).

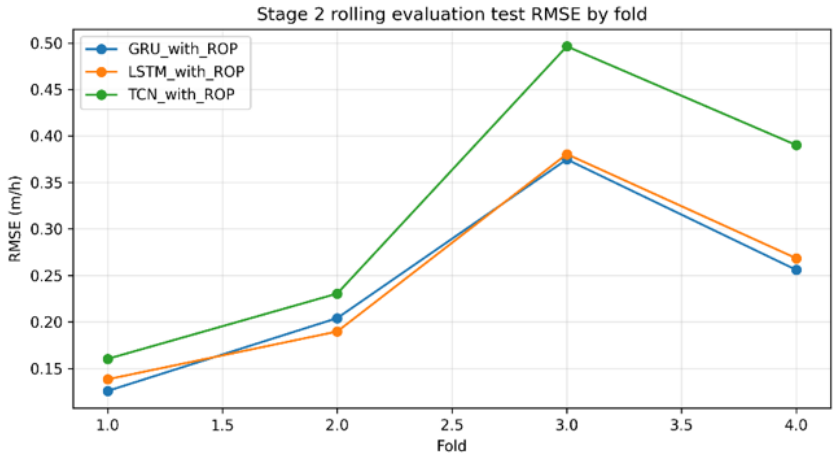

Figure 6. *Stage 2 rolling evaluation test RMSE by fold for LSTM, GRU and TCN.*

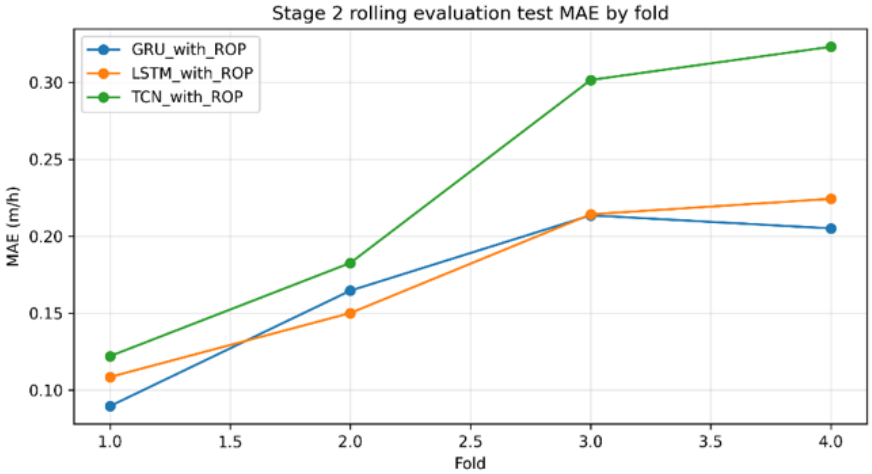

Figure 7. *Stage 2 rolling evaluation test MAE by fold for LSTM, GRU and TCN.*

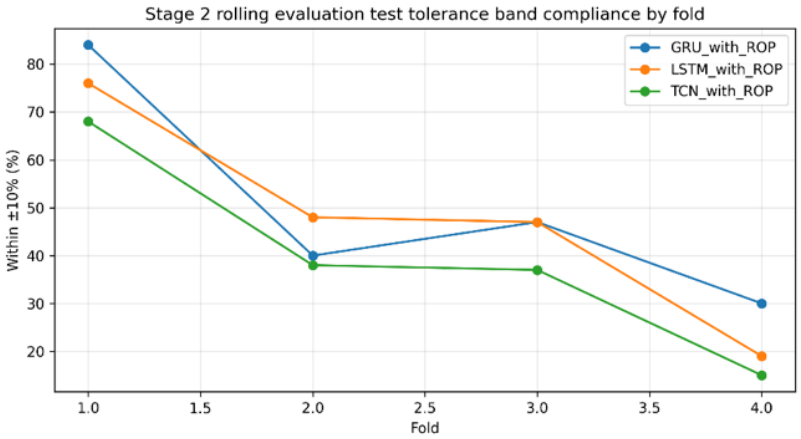

Figure 8. *Stage 2 rolling evaluation test tolerance band compliance within plus or minus ten percent by fold for LSTM, GRU and TCN.*

Table 8. *Top ranked recurrent configurations after lightweight optimization evaluated by rolling mean RMSE MAE and tolerance band compliance.*

Model	Parameter				RMSE (m/h)	MAE (m/h)	Within ±10% (%)
	W	H	D	L			
GRU	10	32	0.2	1e-3	0.229	0.157	53.75
GRU	10	32	0.1	5e-4	0.230	0.155	53.50
GRU	10	32	0.2	5e-4	0.238	0.167	50.00
GRU	20	32	0.1	5e-4	0.239	0.164	49.25
LSTM	20	32	0.2	1e-3	0.240	0.166	50.75
GRU	20	32	0.2	5e-4	0.242	0.168	51.50

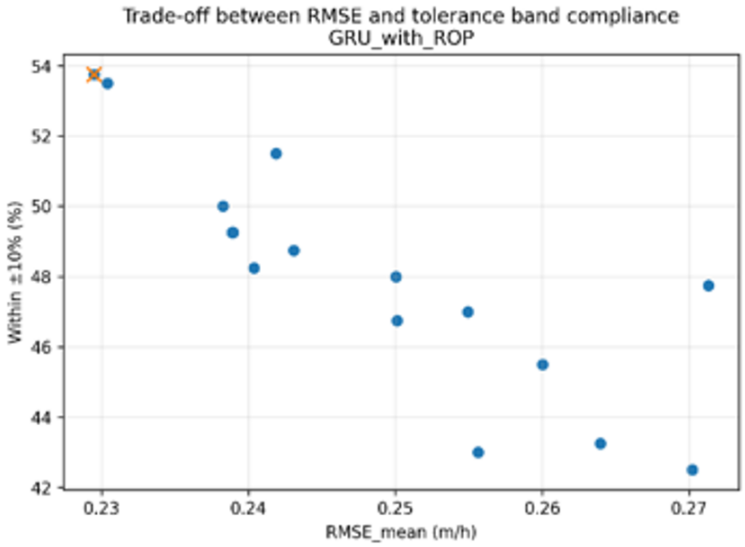

Figure 9. *Trade-off between mean test RMSE and mean tolerance band compliance within plus or minus ten per-cent across lightweight hyperparameter configurations with GRU.*

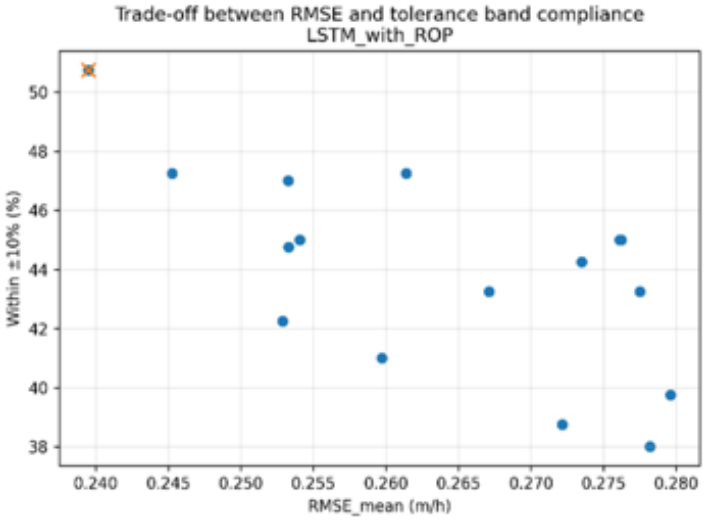

Figure 10. *Trade-off between mean test RMSE and mean tolerance band compliance within plus or minus ten per-cent across lightweight hyperparameter configurations with LSTM.*

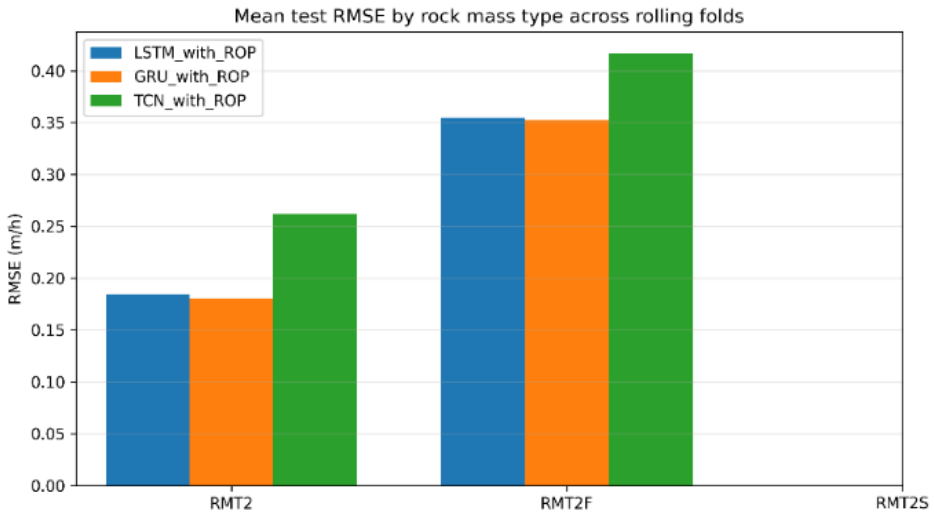

Figure 11. Mean test RMSE by rock mass type across rolling folds for LSTM GRU and TCN.

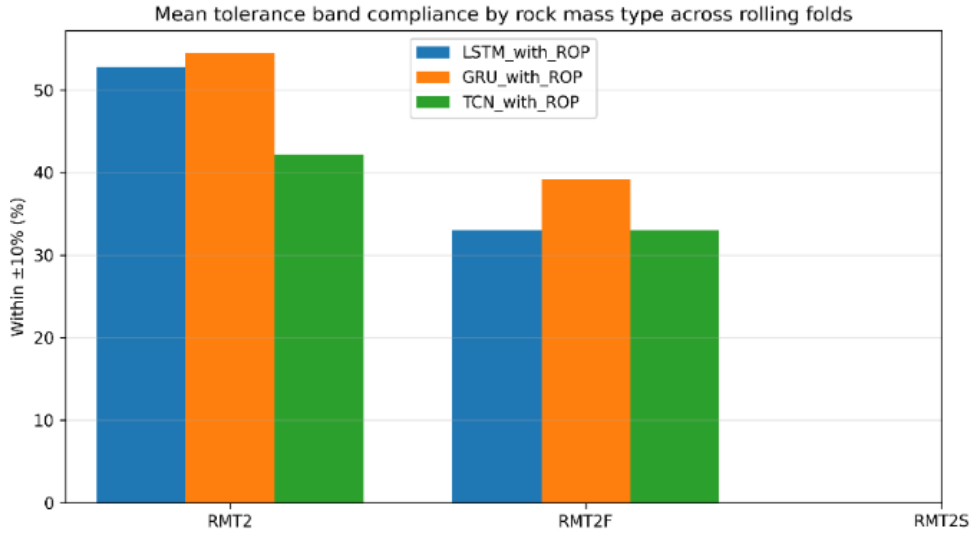

Figure 12. Mean tolerance band compliance within plus or minus ten percent by rock mass type across rolling folds for LSTM GRU and TCN.

6. Discussion

The rolling evaluation results demonstrate pronounced non stationarity of ring scale penetration rate prediction along chainage. Figure 3 and Figure 6 to Figure 8 show that both error metrics and tolerance band compliance vary substantially across successive test blocks, indicating that model reliability is segment dependent under evolving rock mass conditions and operational regimes. The expanding rolling design therefore provides a more defensible construction phase assessment than a single train test split because it repeatedly evaluates generalization on later segments under changing regimes.

Rock mechanics interpretation is supported by regime aware reporting. Table 3 and Figure 11 and Figure 12 indicate that prediction reliability differs between granite dominated rings and discontinuity-controlled regimes, consistent with the expected influence of fracturing and faulting on penetration response. Representative field observations in Figure 4 support the qualitative distinction between intact, highly fractured, and fault influenced conditions, while Figure 5 contextualizes the origin of UCS gaps that motivate Scenario A completion. The limited representation of faulted granite within the analyses interval requires cautious interpretation for RMT2S, but retaining this class provides an explicit placeholder for fault influenced behavior in the framework.

The tolerance band criterion complements RMSE and MAE by providing an engineering interpretable indicator of prediction reliability. Reporting within band compliance by fold and by rock mass type enables a clearer view of where predictions remain within acceptable bounds during excavation, rather

than relying on a single global accuracy statement. The tolerance band is adapted from accuracy band concepts used in AACE based project controls [9]. Future work will extend the framework to more operational settings by introducing causal strength estimation based solely on information available behind the cutterhead and by defining a forward prediction reliability horizon under incomplete geological information.

7. Conclusion

The rolling evaluation results demonstrate pronounced non stationarity of ring scale penetration rate prediction along chainage. Figure 3 and Figure 6 to Figure 8 show that both error metrics and tolerance band compliance vary substantially across successive test blocks, indicating that model reliability is segment dependent under evolving rock mass conditions and operational regimes. The expanding rolling design therefore provides a more defensible construction phase assessment than a single train test split because it repeatedly evaluates generalization on later segments under changing regimes. This paper presented a construction phase prediction framework for hard rock TBM penetration rate using expanding rolling window evaluation under Scenario A UCS completion. The staged results show that rolling evaluation reveals segment dependent prediction reliability under non stationarity and supports regime aware interpretation across granite, highly fractured granite, and faulted granite conditions. Under lightweight optimization, a GRU configuration with a 10-ring input window, 32 hidden units, dropout 0.2, and learning rate 1e-3 was identified as the top ranked model, achieving mean test RMSE 0.229 m/h, mean test MAE 0.157 m/h, and mean within band compliance 53.75 percent across rolling folds. The proposed framework provides a transparent basis for construction phase model selection using both conventional error metrics and an engineering-oriented tolerance band indicator.

Abbreviations

TBM	Tunnel Boring Machine
ROP	Rate of Penetration
RMSE	Root Means Square Error
MAE	Mean Absolute Error
RMT	Rock Mass Type
RMT2	Granite (Massive)
RMT2F/2S	Highly Fractured Granite/Faulted Granite
LSTM	Long Short-Term Memory
GRU	Gated Recurrent Units
TCN	Temporal Convolution Networks

Acknowledgments

The author would like to express sincere gratitude to Chiang Mai University for providing academic support throughout this research. The author also acknowledges the technical background and project information associated with the Mae Tang–Mae Ngad/Mae Kuang Water Transfer Tunnel Project, which contributed to the development and validation of the proposed framework.

Author Contributions

Nantapol Monthanopparat: Conceptualization, Data curation, Formal Analysis, Methodology

Tawatchai Tanchaisawat: Supervision, Validation

Conflicts of Interest

The authors declare no conflicts of interest.

References

[1] Paraskevopoulou C & Boutsis G, Cost overruns in Tunnelling Projects: Investigating the impact of geological and geotechnical uncertainty using case studies, infrastructures, 2020. https://doi.org/10.3390/infrastructures5090073

[2] Pandey P. K. et al., Influence of geology on tunnel boring machine perfromance - A review, Journal of Mining and Metallurgy, pp. 1-14, 2020.

[3] Rostami J., Performance prediction of hard rock Tunnel Boring Machine)TBMs(in difficult ground, Tunnelling and underground space technology, no. 57, pp. 173-182, 2016. https://doi.org/10.1016/j.tust.2016.01.009

[4] Farrokh E. et al., Study of various models for estimation of penetration rate of hard rock TBMs, Tunnelling and Underground Space Technology incorporating Trenchless Research, no. 30, pp. 110-123, 2012. https://doi.org/10.1016/j.tust.2012.02.012

[5] Macias F., Hard rock tunnel boring: performance predictions and cutter life assessment, PhD thesis, Norwegian University of Science and Technology, Faculty of Engineering Science and Technology, Department of Civil and Transport Engineering, 2016.

[6] Monthanopparat N & Tanchaisawat T, Advance Tunnel Boring Machine Performance Prediction in Massive and Highly Fractured Granite: Integrating Innovative Deep Learning and Block Model Technique, Geotechnical Engineering Journal of the SEAGs & AGSSEA, vol. 55, no. 3, pp. 26-34, 2024. https://doi.org/10.14456/seagj.2024.17

[7] Koopialipoor M et al., Development of a new hybrid ANN for solving a geotechnical problem related to tunnel boring machine performance, Engineering with Computers, no. 36, pp. 345-357, 2020. https://doi.org/10.1007/s00366-019-00701-8

[8] Poniewierski J, Block Model Knowledge for Mining Engineers - An Introduction, ACADEMIA, 2019.

[9] AACE, TCM Framwork: 7.3 - Cost Estimating and Budgeting, in COST ESTIMATE CLASSIFICATION SYSTEM - AS APPLIED IN ENGINEERING, PROCUREMENT, AND CONSTRUCTION FOR THE PROCESS INDUSTRIES, 2005.

[10] Rostami J, Development of a force estimation model for rock fragmentation with disc cutters through theoretical modeling and physical measurement of crushed zone pressure, PhD thesis dissertation, Colorado School of Mines, Golden, Colorado, USA, 1997.

[11] Yagiz S, Development of rock fracture and brittleness indiced to qualify the effects of rock mass fracture and toughness in the CSM model basic penetration for hard rock tunnelling machines, thesis, Colorado School of Mines, Golden, Colorado, USA, 2002.

[12] Yagiz S, TBM performance prediction based on rock properties, EUROCK, 2006.
https://doi.org/10.1201/9781439833469.ch97

[13] Bruland A, Vol. 7: The Boring Process, in Hard rock tunnel boring, Trondheim, Norway, Norwegian University of Science and Technology, Department of Building and Construction Engineering, 2000.

[14] Gerhing K, Leistungs- und Verschleiβprognose im maschinellen Tunnelbau, Felsbau Magazin,no. 13, 1995.

[15] Wilfing L, The influence of geotechnical parameters on penetration prediction in TBM tunelling in hard rock, PhD, Technische Universität München, 2016.

[16] Kaewkongkaew K. et al., Geologcal model of Mae Tang-Mae Ngad Diversion tunnel project, Northern Thailand, Open Journal of Geology, no. 3, pp. 340-351, 2013.
https://doi.org/10.4236/ojg.2013.35039

[17] Hewamalage H et al., Forecast evaluation for data scientists: common pitfalls and best practices, Data Mining and Knowledge Discovery, vol. 37, pp. 788-832, 2023.
https://doi.org/10.1007/s10618-022-00894-5

[18] Hochreiter S & Schmidhuber J, Long Short-Term Memory, Neural Computation, vol. 9, no. 8, pp. 1735-1780, 1997.
https://doi.org/10.1162/neco.1997.9.8.1735

[19] Cho K et al., Learning Phrase Representations using RNN Encoder-Decoder for Statistical Machine Translation, in Proceedings of the 2014 Conference on Empirical Methods in Natural Language Processing)EMNLP(, Association for Computational Linguistics, 2014, pp. 1724-1734.
https://doi.org/10.3115/v1/D14-1179

[20] Bai S et al., An Empirical Evaluation of Generic Convolutional and Recurrent Networks for Sequence Modeling, 2018.
https://doi.org/10.48550/arXiv.1803.01271

Biography

Nantapol Monthanopparat is a Ph.D. candidate in Civil Engineering at Chiang Mai University, Thailand. His research focuses on hard rock tunnel boring machine performance prediction, geotechnical data integration, and construction-phase decision support using machine learning and deep learning techniques. His doctoral research develops a construction-phase prediction framework for ring-scale TBM penetration rate in granite formations, incorporating sequence deep learning, inverse distance weighting-based UCS completion, rolling-window evaluation, and reliability monitoring. He has experience in tunnel engineering, underground construction, and geotechnical engineering, particularly in relation to water transfer tunnel projects in Northern Thailand. His research has been applied to the Mae Tang–Mae Ngad/Mae Kuang Water Transfer Tunnel Project. His broader interests include TBM operation, rock mass characterization, construction data analytics, and sustainable underground infrastructure development.

Research Field

Nantapol Monthanopparat: Hard Rock Tunnelling, Rock Mechanics, Rock Supporting, Tunnel Boring Machine, Project Management